3D Shape Modeling for Hearing Aid Design

Greg Slabaugh, Tong Fang, Fred McBagonluri, Alexander Zouhar,
Rupen Melkisetoglu, Hui Xie, Gozde Unal

According to recent estimates, hearing loss affects approximately 314 in 1000 adults over the age of 65. While there are many causes of hearing loss, including genetic factors, disease, trauma, and exposure to damaging noise, the most common treatment is a hearing aid. Since a patient typically uses a hearing aid for many hours during the day, it must be comfortable to wear. Hearing aids are typically custom-made to match the three-dimensional (3D) geometry of the patient's ear in order to achieve a comfortable fit.

This article presents a software-based approach to interactive 3D shape modeling for geometric design of hearing instruments. We review various shape modeling operations that transform a raw impression to the final shape of the hearing aid device. In addition, we present state-of-the-art methods for automating the design process.

HEARING AIDS

Anatomical Perspective

When designing a hearing aid, surface manipulations are often carried out with respect to anatomical features of the ear. In Figure 1 (a) and (b), we simultaneously an image of a right ear along with an impression (described below) to show the major relevant features. The *canal* is top-most portion of the surface and is the part that goes inside the ear canal. The *aperture* is a plane that separates the inner ear and the outer ear. The *tragus* is the small flap of cartilage near the aperture. Across from the tragus is the *anti-tragus*. The tragus and anti-tragus are protrusions of the ear geometry so they appear as indentations on the impression. Between the tragus and anti-tragus is the *notch*. Also near the aperture, the *concha* is the bowl-shaped cavity that appears as a hump on the impression. The *crus* is a ridge of cartilage on the ear and appears as a valley on the impression. The *cymba* is an indented region next to the crus, while the *anti-cymba* is the flap of cartilage above the cymba in the picture of the ear. On the impression, the cymba is a protrusion and the anti-cymba is an indentation. Please see Gray's anatomy [1] for more details.

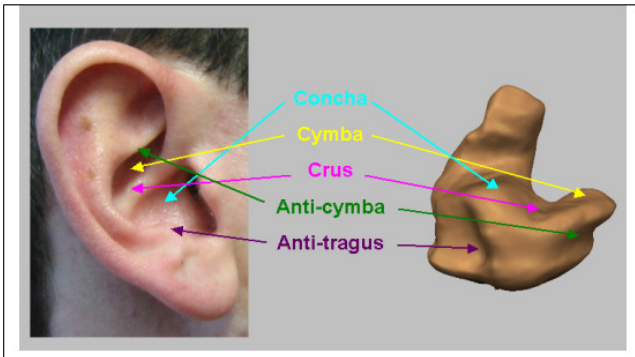

(a)

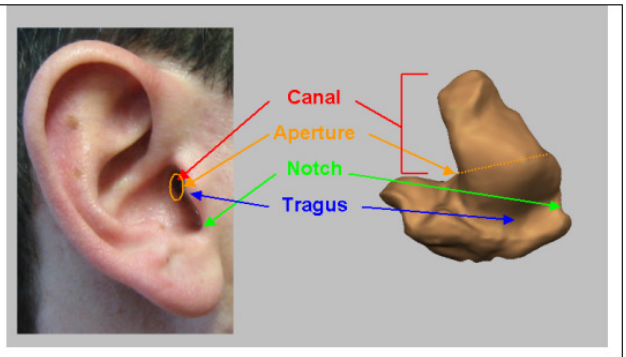

(b)

Figure 1. Major anatomical features of the outer ear.

Engineering Perspective

Hearing aid design is complex, as each patient has different ear geometry, and based on the extent of the patient's hearing loss, different electronic components are required. As a result, hearing aids come in a variety of types, as shown in Figure 2, including completely in the canal (CIC), in the canal (ITC), and in the ear (ITE) devices. For discretion, patients who experience hearing loss typically prefer CIC hearing aids. However, more severe loss requires larger hearing aids to house larger electronic components.

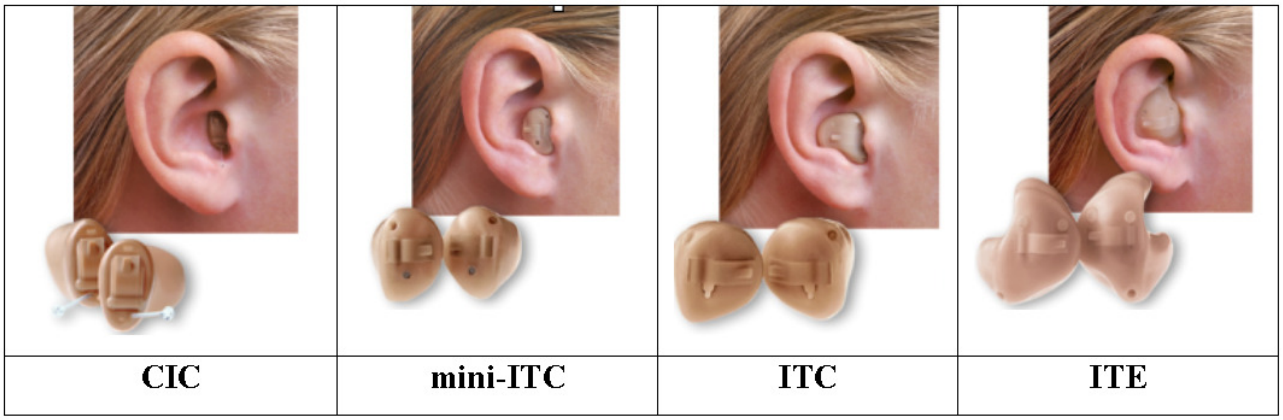

CIC | mini-ITC | ITC | ITE

Figure 2. Different types of hearing aids. From left to right: CIC, mini-ITC, ITC, ITE.

Design and manufacturing

Historically, hearing aids were made through a tedious manual process that was highly operator dependent and error-prone. Within the last five years, advances in 3D scanning technologies, computational geometry, and layered manufacturing have dramatically transformed

hearing aid manufacturing. Today, a large percentage of hearing aids are produced using software-based systems. The process begins at an audiologist's office, where thermosetting material is placed into the patient's ear. The material hardens, taking the shape of the patient's ear, and is removed. This mold, or *impresion*, is then scanned using a projected light scanner, which captures the 3D impression geometry as a point cloud, sent electronically to the manufacturing site. The impression is loaded into 3D design sofware and the surface is processed in two steps: detailing, and modeling, described below. The final surface is output as a stereo-lithography (STL) file, which is then built into a physical model a layered manufacturing system. After the electronic components are added and the hearing aid is tested for quality assurance, the final product is shipped to the customer. The block diagram for the overall process appears in Figure 3.

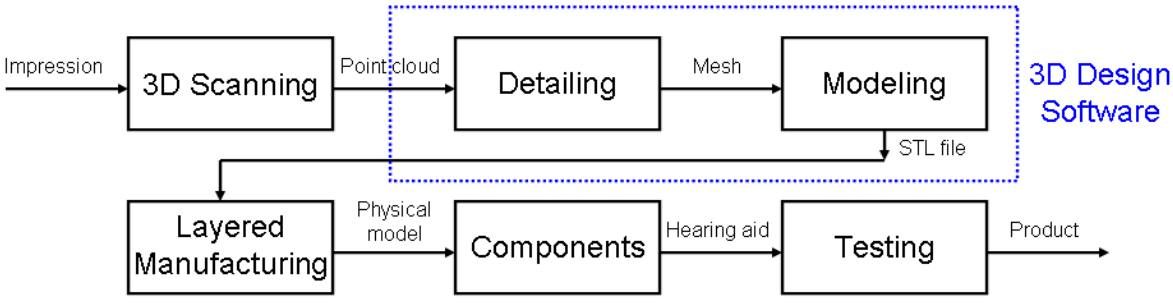

Figure 3. Overall block diagram for hearing aid manufacturing, from the impression to the final product. This article considers the 3D Design Software in the dotted box.

Challenges

There are numerous challenges facing the design and development of 3D hearing aid software. First, ear geometry vary dramatically from person to person, and therefore the software must be robust to this variation. The final device should be as small as possible and must fit inside the original impression. Since existing tools are interactive, computational performance is critical so that operators do not wait significantly when working with the data.

Previous work

Previous attempts to apply computed-aided design (CAD) principles hearing instrument design relied on multiple general-purpose 3D software systems, including Parasoid and CATIA. Such approaches took approximately 20-25 minutes to model one complete hearing instrument. Subsequently, hearing-aid specific software, like Materialise MagicsRSM addressed the modeling part but did not have suitable functionality for detailing. This paper is based on AutoMoDe, the

first all-encompassing detailing and modeling technology with an artificial intelligence basis for hearing instrument design [4].

SIGNAL PROCESSING OF 3D SHAPES IN HEARING AID DESIGN

We begin with a description of the detailing operations, which reduce the impression to the shape of the hearing aid as depicted in Figure 4.

Detailing

Triangulation and topology correction

The first step of the detailing process is surface reconstruction, which transforms the point cloud into a polygonal mesh, which is easily rendered with graphics hardware and supports queries about neighborhood geometry. Surface reconstruction is a classic problem in computer graphics, and several well known solutions exist, including power crust [1] and ball pivoting [2]. After triangulation (Fig. 4a), it is possible that small holes exist on the surface. Holes are easy to locate, since at a hole an edge connecting two vertices will only be part of one face. By grouping such edges together, connected hole contours are detected and then filled using constrained Delaunay triangulation (Fig. 4b). After hole filling, the resulting surface is a two-manifold with a boundary at the base of the surface.

Interactive Surface Manipulation Tools

In the detailing process, interactive surface manipulation tools allow the operator to transform the surface into a hearing aid shape.

Smoothing tools

Smoothing is available at any time in the detailing process. Smoothing tools rely on a Laplacian smoothing algorithm that is sensitive to the convexity of the surface. In particular, they locally deform mesh vertices using the equation

$$\frac{\partial \mathbf{v}_i}{\partial t} = \chi_i \lambda_i \mathbf{L}_i, \qquad (1)$$

where $\mathbf{v}_i$ is a mesh vertex to be smoothed, λ_i is a diffusivity coefficient that controls the degree of smoothing,

$$\mathbf{L}_i = \frac{1}{M} \sum_{j \in N(i)} \mathbf{v}_j - \mathbf{v}_i \qquad (2)$$

is the discrete Laplacian operator that determines a displacement $\mathbf{L}_i$ using the M vertices $\mathbf{v}_j$ in the (one-ring) neighborhood of $\mathbf{v}_i$, and

$$\chi_i = \begin{cases} 1, & \mathbf{L}_i \cdot \mathbf{N}_i < 0 \\ 0, & \text{otherwise} \end{cases} \quad (3)$$

is an indicator function that determines if the displacement is inward using $\mathbf{N}_i$, the surface normal at $\mathbf{v}_i$. Outward displacements are avoided to ensure the deformed surface fits inside the original impression. Note that Equation 1 is simply a discretized form of the heat equation. By integrating this equation over time, the high frequencies on the mesh become dispersed, while the main surface shape, represented by the lower frequencies, is largely unaffected.

Cutting tools

The bottom of the impression is cut with a plane that passes through the tragus, anti-tragus, and anti-cymba, (Figs. 4c and 4d). For ITE models, this defines the length of the hearing aid. Then, the canal is tapered at the tip (Fig. 4e), using cutting and Laplacian smoothing. For ITE devices, a cut is applied to remove part of the cymba, while for CIC and ITC devices, a cut applied at the crus completely removes the cymba (Fig. 4f). Using the Laplacian smoothing algorithm, local inward deformations are applied along the crus in for ITE. Finally, for CIC devices, a cut is applied at the aperture so that the device is completely in the canal (Fig. 4g).

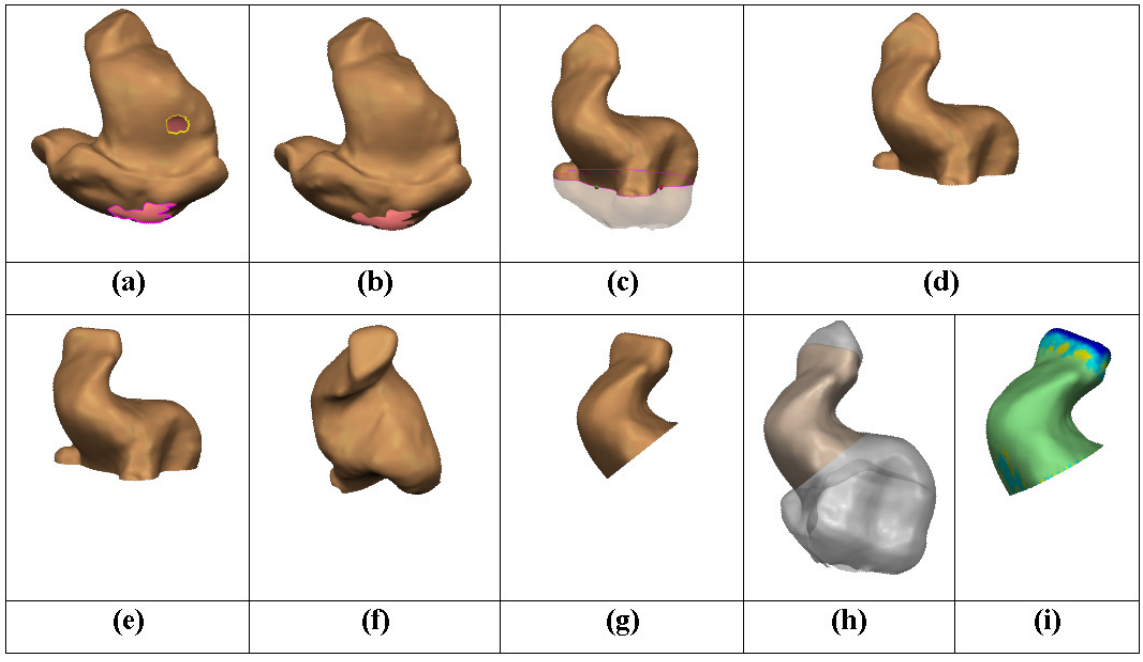

Figure 4. Surface detailing process. See text for description.

Virtual cast and color mapping

The software can provide a virtual cast, which renders the original impression transparently along with the detailed surface (Fig. 4h). With this visualization, the operator can check the quality of the detailed surface, as well as visualize the distance between the detailed shape and the impression (Fig. 4i). Distance queries between a vertex on the detailed surface and the impression surface are efficiently processed using a k-d tree [5].

Modeling

After detailing, the surface has the shape of a hearing aid. The modeling process, depicted in Figure 4, considers the components that are placed inside the device.

Thickness and vent

The first step of modeling is to add thickness, which is typically uniform and achieved by computing an offset surface (inner wall) from the surface from detailing (outer wall). A connecting surface stitches the inner wall and outer wall together, and topologically, the resulting surface S is a manifold without boundary (Fig. 5a). The next step is to add a vent, which is a tubular structure that runs the length of the hearing aid. The vent allows air to pass through the hearing aid so that when inserted, the air pressure inside the patient's ear canal will match the ambient air pressure outside the ear. A surface path is determined on the outer wall using a curvature-weighted geodesic algorithm between a point on the canal tip and on the base of the impression (Fig. 5b). From this path, two tubular surfaces are generated, forming an inner wall I, and an outer wall O of the vent. Using Boolean operations, the vent is attached, shown in Fig. 5c, using $S' = (S - I) \bigcup O$, where "–" is a mesh difference operator and "$\bigcup$" is a mesh union operator. Boolean operations permit logical combinations of meshes.

Components and labeling

The hearing aid contains several components, including a battery, microphone, amplifier, receiver, and faceplate. The receiver converts the amplified electrical signal into an acoustic signal for transmission into the ear. It is desirable to place the receiver as far up the canal as possible. However, the geometry of the surface limits the receiver placement. An automatic receiver placement tool searches the 6D space of translations and rotations of the receiver and places the receiver at its optimal location and orientation, as shown in Fig. 5d. A 3D text label is applied to the inner wall of the surface for later identification of the device. Labeling is achieved by using Windows path functions to determine 2D letter geometry and a 3D surface is extruded and merged

with Boolean operations onto the surface (Fig. 5e and 5f). If the receiver touches the inner wall of the surface or label, the surface is locally deformed to accommodate the components.

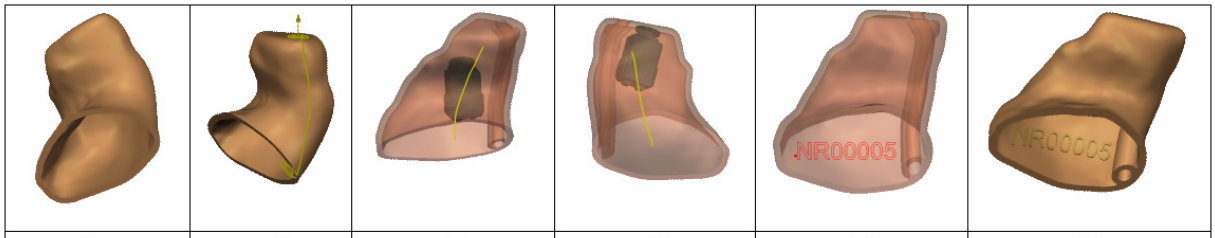

(a) (b) (c) (d) (e) (f)

Figure 5. Modeling process. See text for description.

AUTOMATION OF DETAILING AND MODELING

Automating the design of hearing aids increases operator efficiency as well as the reproducibility of design.

Binaural processing

A large percentage of patients experiencing hearing loss require two hearing aids; one for the left ear and another for the right. Typically, the left and right ear impressions are largely symmetric with mirror symmetry. Therefore, binaural processing allows an operator to apply detailing and modeling operations on a left (right) impression, and automatically have the operations applied with mirror-symmetry to the right (left) impression. This requires accurate registration between the impressions. First, one mesh is transformed to have mirror symmetry, by multiplying all vertices by a matrix $M = \begin{bmatrix} -1 & 0 & 0 \\ 0 & 1 & 0 \\ 0 & 0 & 1 \end{bmatrix}$. Then, registration between two shapes can be achieved using iterated closest points (ICP). For proper convergence, ICP requires a good initial alignment. One way to estimate the initial rotational alignment is to construct extended Gaussian images (EGIs) [6], which are translation-independent orientation histograms formed over $\alpha = [\theta, \phi]\text{^}T$ by binning a mesh's surface normals in spherical bins. Two EGIs can then be efficiently cross-correlated to estimate the rotational shift that brings them into alignment using

$$G(R) = \iint H_1(\alpha) H_2(R^T \alpha) d\theta d\phi, \qquad (4)$$

where $R \in SO(3)$ is a rotation in the Lie group of rotations about the origin of 3-dimensional Euclidean space, and H_1 and H_2 are the EGIs of the two surfaces. Using the spherical Fourier

transform [3], Equation 4 can be efficiently implemented in the frequency domain. The peak of G(R) indicates the rotational shift that will align the two meshes. Then, to estimate the translational alignment, a similar procedure is formed using 3D histograms formed in x, y, z and the standard cross-correlation operator, also implemented in the frequency domain, but using the standard 3D Fourier transform.

Feature recognition

Most of the operations applied in detailing and modeling are based on the anatomic features of the ear impression. Therefore, automatic recognition of these features enables automation of detailing and modeling. One way to recognize features is through analysis of contours that intersect parallel planes running through the shell. For example, the aperture can be detected by looking for a large increase in contour area going from the canal tip to the base of the impression. Any triangles above the aperture are part of the canal. Forming a polyline through the contour centroids gives a rough centerline. The tragus, anti-tragus, and anti-helix can be found by studying the curvature of contours near the base of the impression. Other features can be found using similar geometric analysis. See Figure 6 (a) and (b) for an example.

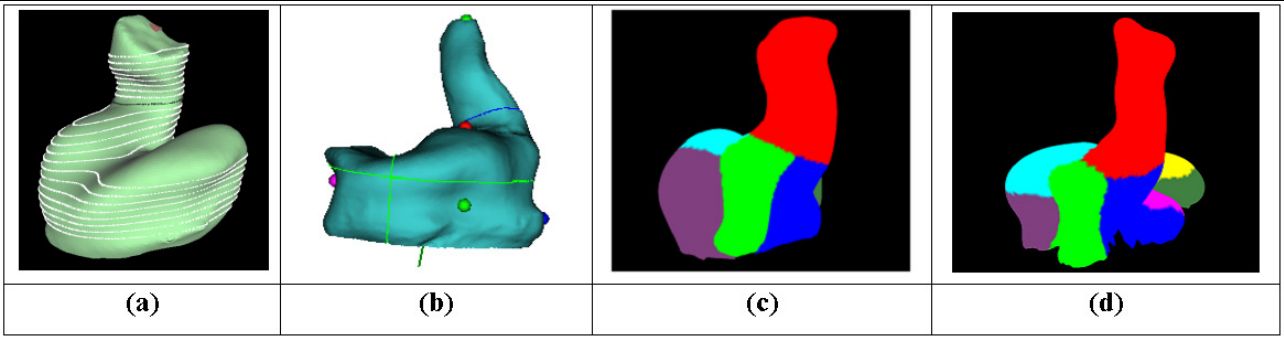

Figure 6. Feature detection and surface segmentation. Contours generated from slicing planes (a) and analyzed in (b) to find the canal tip (top most point), aperture (blue contour), concha (red point), anti-tragus (green point near bottom), anti-cymba (purple point). Atlas surface (c) and automatically segmented surface (d). Colors correspond to those in Figure 1.

Surface segmentation

Feature recognition determines individual points or planes. However, sometimes regional information of impression is useful. Surface segmentation determines a unique label for each vertex on the impression. This can be achieved by using a manually labeled atlas. Vertices on an

unlabeled surface are compared using a shape descriptor, such as the shape context [7] (log polar spherical histogram of points), to vertices on the labeled atlas. In this way, the labels from the atlas can be transferred to the new surface. See Figure 6 (c) and (d) for an example.

Outlook

Advances 3D scanning and fabrication hardware as well as 3D geometric design software have transformed a once labor-intensive manual manufacturing into an efficient digital process for hearing aid design, resulting in higher quality, reduced cost, and better fitting devices. Future work in this field will continue to focus on increasing automation until the process is fully automatic.

Greg Slabaugh, greg.slabaugh@gmail.com, is a Project Manager at Siemens Corporate Research in Princeton, New Jersey.
Tong Fang, tong.fang@siemens.com, is a Program Manager at Siemens Corporate Research.
Fred McBagonluri, fred.mcbagonluri@siemens.com, is the Director of Research and Development at Siemens Hearing Instruments in Piscataway, New Jersey.
Rupen Melkisetoglu, rupen.melkisetoglu@siemens.com, is a Research Scientist at Siemens Corporate Research.
Alexander Zouhar, alexander.zouhar@siemens.com, is a Research Associate at Siemens Corporate Research.
Gozde Unal, gozdeunal@sabanciuniv.edu, is an Assistant Professor at Sabanci University in Istanbul, Turkey.

References

[1] Nina Amenta, Sunghee Choi and Ravi Kolluri, "The power crust, unions of balls, and the medial axis transform," *Computational Geometry: Theory and Applications*, 2001, 19:(2-3), pages 127-153.

[2] F. Bernardini, J. Mittleman, H. Rushmeier, C. Silva, and G. Taubin, "The Ball-Pivoting Algorithm for Surface Reconstruction," *IEEE Transactions on Visualization and Computer Graphics*, 5(4):349-359, 1999.

[3] P. J. Kostelec and D. N. Rockmore, "FFTs on the Rotation Group," *Santa Fe Institute Working Papers Series* Paper #03-11-060, 2003.

[4] Martin Masters, Therese Velde and Fred McBagonluri (2006), “Rapid Manufacturing in the Hearing Industry, *In Rapid Manufacturing Technologies: The Next Industrial Revolution,”* Eds. Neil Hopkinson, Richard Hauge (Editor), Phillip Dickens, Rupert Soar. John Wiley and Sons; New York, NY.

[5] Cormen, T. H., Leiserson, C. E., Rivest, R. L., *Introduction to Algorithms*. The MIT Press; 2nd Edition, 2001.

[6] A. Makadia, A. Patterson, and K. Daniilidis, “Fully Automatic Registration of 3D Point Clouds,” Proc. CVPR 2006.

[7] S. Belongie, J. Malik, and J. Puzicha, "Shape Matching and Object Recognition Using Shape Contexts," IEEE Transactions on Pattern Analysis and Machine Intelligence, 2002.